ALONGSHORE BED LOAD TRANSPORT ON THE SHOREFACE AND INNER SHELF

M.G. Kleinhans and B.T. Grasmeijer
(Utrecht University)

ABSTRACT

Bed load transport rates on the shoreface and shelf are determined by tidal currents, wave-current interaction and grain size. There is, however, a strong lack of field data and validated models because bed load transport under waves cannot be measured in the field, while bed load transport by currents without waves commonly is barely measurable in spring tidal conditions. Herein, bed load transports were carefully measured with a calibrated sampler in spring tidal conditions without waves at a water depth of 13-18 m in fine and medium sands at 2 to 8.5 km offshore the Dutch coast. Near-bed flow velocity was recorded at 2 Hz. The measurements are used to derive an empirical bed load model, in which transports are normalized by grain size and density. The model produces bed load transports that are at least a factor 5 smaller than predicted by existing models. However, they agree with a large laboratory data set of sand and gravel transport in currents near incipient motion. Cohesion of sediment due to mud in-mixing or biological activity was excluded. Including turbulence probabilistically in bed load models strongly improves predictions near incipient motion, and predict 20% more alongshore transport annually for currents only. The effect of wave-current interaction is predicted to be twice as large, and the combined effect results in 100% larger transports. The effect of wave stirring is gives much larger flood and ebb transports but the net transport is the same as for the combined wave-current interaction and turbulence case. An overestimation of the current velocity leads to much larger transports than any of the model combinations. Concluding, the effects of turbulence, wave-current interaction and wave stirring are of secondary importance compared to the choice of empirical or existing bedload predictor and the representation of the current climate.

1. INTRODUCTION

A better understanding is needed of the sediment dynamics on the shoreface for sand mining and long-term coastal development purposes (introduction of this volume). An important part of the total alongshore sediment transport is driven by tidal currents. In currents only, commonly the bed shear stress is near the critical Shields parameter for incipient motion for a large proportion of the tidal cycle. Thus, the bed load transport is low, but since this is the predominant condition throughout the year, it may be significant for the total alongshore sediment transport (Van Rijn, 1997). Moreover, bed load transport in tidal currents is measurable with samplers, while it cannot be measured under waves. Madsen and Grant (1976) and Ribberink (1998) found that bed load predictors for currents can also be applied to conditions with waves or waves plus currents. This means that an empirical bed load predictor based on measurements in tidal current conditions without waves can potentially be applied to conditions with waves. This will be the approach herein. Suspended transport and annual total transport is covered in Grasmeijer et al. (2005, papers B and U).
Most bed load sediment transport predictors are very sensitive to small changes in shear stress near the critical Shields number. This is problematic for an empirical derivation, and will lead to large errors when used for predicting annual sediment transport budgets. Kleinhans and Van Rijn (2002) showed that this sensitivity is largely due to the hard criterion for incipient motion, while in reality the turbulent fluctuations of the flow make the criterion gradual. By including a stochastic description of turbulence, significant transports are predicted even if the average shear stress is below the critical Shields number.
The objective of this paper is to compare the effects of turbulent fluctuations, wave-current interaction, wave stirring and current climate on alongshore bed load transport at a water depth of 10-20 m. We present (1) field data of directly measured tidal bed load transport rates, (2) empirical values of critical shear stress, (3) a test of bed load prediction methods including one that accounts for the near-bed turbulence, and (4) an estimate of the effect of wave-current interaction and wave stirring on bedload transport and the effect of using a different current climate (of Van Rijn, 1997).

2. FIELD SITE AND METHODOLOGY

The field sites are on the Dutch shoreface and shelf in the North Sea, 2 and 8.5 km off Noordwijk at an average water depth of 13 and 18 m. Tidal currents are semi-diurnal. The spring-tidal amplitude is 1.3 m and maximum tidal depth-averaged currents are between 0.5-0.7 m s^{-1}. The bed sediment is fine to medium sand (Table 1).
The hydrodynamics were measured by 3 to 7 electromagnetic current sensors between 0.05-1m above the bed and a pressure sensor on a nearby tripod (only for the 2.2 km offshore data), and with one or two OTT

propellor type current meters on the bed load sampler. In the Van de Meene data the velocities were measured with 3 OTT current propellors on the sampler. In addition, 1 year (>8000 hours) of data was collected with an electromagnetic current sensor at a height of 0.32 m above the bed on a separate tripod ('Hydro tripod') at 2 km offshore between March 2003 and March 2004. The latter data is used to compute an empirical probability distribution of depth-averaged current velocity and orbital velocity of the 1/3 largest waves. All instruments operated in burst mode with a frequency of 2 Hz and a burst duration of 34 minutes.

Table 1 *Bed load sampling campaigns.*

Date	site	depth (m)	km offshore	location	D_{10} (μm)	D_{50} (μm)	D_{90} (μm)
14 August 1991	Zandvoort	14	7.3	top shoreface-connected ridge	244	280	336
5 March 2003	Noordwijk	13	2.2	shoreface	160	216	288
25 Sept 2003	Noordwijk	13	2.2	shoreface	185	227	305
6 Nov 2003	Noordwijk	18	8.5	top sandwave	227	273	347

The bed load transport rate was measured with a basket-type bed load 'Nile' sampler during two spring-tidal flood peaks and one ebb peak. This sampler has a nozzle of 0.095 m wide and 0.05 m high with a nylon sampling bag with mesh 0.15mm, and an OTT current meter at 0.65 m above the bed. The sampler was carefully placed on the bed, and the effect of the landing was quantified independently by measuring the sampled volume after landing and lifting five times with a sampling duration of ~1 second. This zero sampling volume was subtracted from the bed load samples. The sampling durations were between 10 and 40 minutes depending on the current velocity. The calibration factor of the Nile sampler is 1.0±0.3 (Gaweesh and Van Rijn 1994). The suspended load concentrations were measured on 25 September 2003 but remained below 20±15 mg l^{-1} (error is 95% interval) just above the bed load sampler nozzle for the maximum flow velocity and are not reported here. The Nile sampler data of Van de Meene (1994, pers. comm.) of the Zandvoort site are included as well because the method and site are almost the same.

The time- and depth-averaged velocity (u) was determined by a fit to the EMF data assuming a logarithmic velocity profile up to the water surface:

$$u=u^*\kappa^{-1}\ln(z/z_0) \quad (1)$$

in which u*=shear velocity, κ=Karman constant (0.4), z=height above the seabed and z_0=height at which u=0. The depth-averaged flow velocity is found at a height of (1/e)h, where h=water depth and e=Euler constant, which was approximated as 0.368h.

The current shear stress related to grains was computed as

$$\tau_c=\rho g u^2/C^2 \quad (2a)$$

$$\tau_c=0.5\rho f_c u^2 \quad (2b)$$

$$C=18\log(12h/D_{90}) \quad (3)$$

in which ρ=sea water density (1025 kg m^{-3}), g=9.81 m s^{-2}, D_{90}=90% grain size distribution percentile and f_c is discussed below. This assumes hydraulic rough conditions, which is checked as:

$$Re^*=u^*D_{90}/\nu >11.63 \quad (4)$$

in which ν=viscosity.

The wave shear stress related to grains was computed as

$$\tau_w=0.5\rho f_w u_{orb,sig}^2 \quad (5)$$

$$f_w=\exp[5.213(2.5D_{50}/A_{orb,sig})^{0.194}-5.977] \quad (6)$$

in which $u_{orb,sig}=(u_{orbX,sig}^2+u_{orbY,sig}^2)^{0.5}$ significant orbital velocity from orbital velocities measured cross-shore and alongshore, and $A_{orb,sig}$=significant orbital amplitude, here taken from the pressure signal as $A_{orb,sig}=(u_{orb,sig}T_{sig})/2\pi$.

The bed shear stress of interacting waves and currents was computed following Soulsby (1997), assuming that the waves come in perpendicular to the currents:

$$\tau_{cw}=\tau_c\{1+1.2[\tau_w/(\tau_c+\tau_w)]^{3.2}\} \quad (7)$$

in which τ_{cw} = effective grain-related shear stress of the current affected by waves. The maximum shear stress due to waves plus current (wave stirring) must exceed the critical shear stress for motion in order for bed load to occur (Soulsby, 1997) and is computed as:

$$\tau_{cwmax}=[\tau_w^2+\tau_{cw}^2]^{0.5} \quad (8)$$

assuming the wave propagation direction perpendicular to currents.

The wave stirring effect on bedload transport is computed with the method of Ribberink (1998). In this method, the wave-current interaction is incorporated in a wave-current friction factor for the instantaneous (intra-wave) velocity vector:

$$f_{cw}=\alpha f_c+(1-\alpha)f_w \quad (9)$$

in which the wave friction is computed with equation 6. The current friction parameter is computed for the near-bed velocity at height δ, which was determined from the measured velocity at a much larger height, an assumed apparent roughness of 0.1 m and the logarithmic velocity profile (Ribberink, 1998):

$$f_c=2[0.4/\ln(\delta/z0)] \quad (10)$$

in which δ=0.01m is taken here. An instantaneous velocity vector is computed from the time-averaged alongshore current and a cross-shore sine wave with $u_{orb,rms}=2^{(1/2)}u_{orb,sig}$ constructed at 10 Hz with the $T_{1/3}$ of the surface waves. The instantaneous transport is computed from the instantaneous velocity vector and the time-averaged friction factor for waves plus currents, then decomposed into cross-shore and alongshore transport and then averaged over the wave for the alongshore direction.

The dimensionless current or wave shear stress ('Shields parameter') was computed as

$$\theta=\tau/[(\rho_s-\rho)gD_{50}] \quad (11)$$

in which ρ_s=sediment density (2650 kg m^{-3}). The critical Shields parameter was predicted with the analytical model of Zanke (2003), which can be approximated for D<5 mm as:

$$\theta_{cr}=\alpha[0.145D^{*-0.5} + 0.045\ 10^{(X)}] \quad (12)$$

in which $X= -1100D^{*(-9/4)}$, $D^*=D_{50}[(Rg/\nu^2)]^{(1/3)}$ with $R=(\rho_s-\rho)/\rho$ is relative submerged density and α=1 in the original, and 0.5 herein based on earlier comparisons between the Shields criterion (large transport rate) and other measures (smaller transport rate) for incipient motion. For D>5 mm the θ_{cr} is that for 5 mm. The sediment transport is given in nondimensional form ('Einstein parameter') as:

$$\phi= q_s/[R^{0.5}g^{0.5}D_{50}^{1.5}] \quad (13)$$

in which q_s=sediment transport rate in $m^3\ m^{-1}\ s^{-1}$.

The critical dimensionless shear stress for incipient motion was determined empirically in a comparable way of the similarity collapse method of Parker et al. (1982). This method consists of two steps. First, a power function is fitted to the data plotted as Einstein parameter versus Shields parameter. Second, a reference transport rate is chosen (here: $\phi_{ref}=5\ 10^{-4}$) in the order of the lowest measurable transport. The Shields parameter at the intercept of the power function with the reference transport rate is the reference Shields value θ_{ref}, which is similar to, but commonly lower than the critical Shields value θ_{cr}. The original method of Parker (1982) cannot be used for power functions with powers below 1.5.

The bed load sediment transport predictors of Van Rijn (1984), Meyer-Peter and Mueller (1948), Ribberink (1998), Fernandez-Luque and Van Beek (1976) and the Parker et al. (1982) approximation of the Einstein predictor are all of the form:

$$\phi=a(\theta-\theta_{cr})^b \quad (14a)$$

$$\phi=a(\theta/\theta_{cr})^b \quad (14b)$$

$$\phi=a[(\theta-\theta_{cr})/\theta_{cr}]^b \quad (14c)$$

where a,b=empirical constants O(1-10) (Table 2). In Van Rijn (1984) there is also a grain size dependence on D* but that does not vary with shear stress so is essentially a constant for a given sediment.

Table 2 *Bed load predictors.*

predictor	form	a	b	θ_{cr}
Meyer-Peter and Mueller (1948)	$\phi=a(\theta-\theta_{cr})^b$	8	1.5	0.047
Fernandez-Luque and Van Beek (1976)	$\phi=a(\theta-\theta_{cr})^b$	5.7	1.5	0.03
Parker et al. (1982)	$\phi=a(\theta/\theta_{cr})^{b1}/\theta^{b2}$	11.2	4.5/3	from 0.5 Shields
Van Rijn (1984)	$\phi=a[(\theta-\theta_{cr})/\theta_{cr}]^b$	0.1	1.5	from Shields
Ribberink (1998)	$\phi=a(\theta-\theta_{cr})^b$	11	1.65	
Wilson (1987)	$\phi=a(\theta-\theta_{cr})^b$	12	1.5	
Wiberg and Smith (1989)	$\phi=a(\theta-\theta_{cr})^b$	$1.6\ln(\theta)+9.8$	1.5	
North Sea (see text)	$\phi=a(\theta-\theta_{cr})^b$	1	1.5	from Zanke—Shields

It is interesting to note that Wiberg and Smith (1989) provide a variable a depending on θ, which covers the range of a by Fernandez-Luque and Van Beek, Meyer-Peter and Mueller and Wilson. The effect of this could also be expressed as an increased coefficient b while keeping a constant. By fitting, a=9.7 and b=1.67 are obtained for $0.045<\theta<4$ with only 1.5% deviation, which is remarkably close to Ribberink.

For a stochastical approach to turbulence any of the above mentioned predictors can be applied for a range of τ_{ci} below and above the average τ_c. The computed transports ϕ_i are multiplied with the probabilities p_i of occurrence of all the τ_i in the distribution of instantaneous shear stress for each burst. This may be a normal or log-normal distribution parameterised by the average τ_c and the standard deviation s_τ, for example:

$$p_i=\Delta\tau_c[(2p)^{0.5}s_\tau]^{-1}\exp\{-0.5[(\tau_c-\tau_{ci})s_\tau^{-1}]^2\} \quad (13)$$

for the discretised normal distribution. The sum of the products represents the cumulative bed load transport due to turbulent fluctuations (Kleinhans and Van Rijn 2002):

$$\phi=\Sigma p_i\phi_i\tau_c \quad (14)$$

for non-zero transports ϕ_i in both updrift and downdrift direction. This makes the test for wave stirring effects on incipient motion (equation 8) redundant.

3. RESULTS

The velocities measured with different instruments give comparable results (Figure 1). In addition, there is a strong correlation (not shown) between the depth-averaged velocity computed from the logarithmic profile fit and the velocity at one single height of 0.32 m (factor 1.4 smaller than depth-averaged), indicating that the hydraulic roughness does not have much effect on the depth-averaged current. The bed was nearly plane with rounded and scoured relic bedforms during all measurements.

The instantaneous flow velocities are used only to derive the probability distribution of grain shear stresses. The empirical probability distribution of velocity fitted well to a normal distribution. The instantaneous τ' were lognormally distributed with standard deviations of 0.28 times the average τ. For fluvial conditions this is known to be about 0.4 (Kleinhans and Van Rijn 2002) from measurements with a high enough frequency to cover the full turbulence spectrum, whereas herein the sampling frequency was low, so 0.4 is assumed.

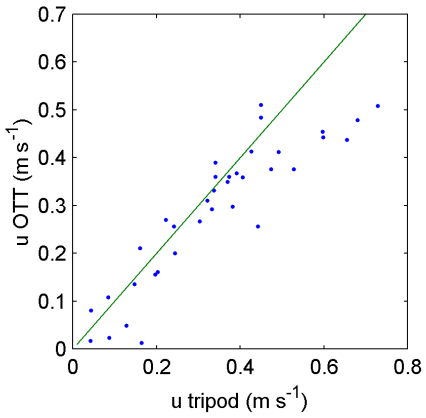

Figure 1 *Comparison of Ott current meter at z=0.56 m and depth-averaged velocity from the EMF's on the tripod.*

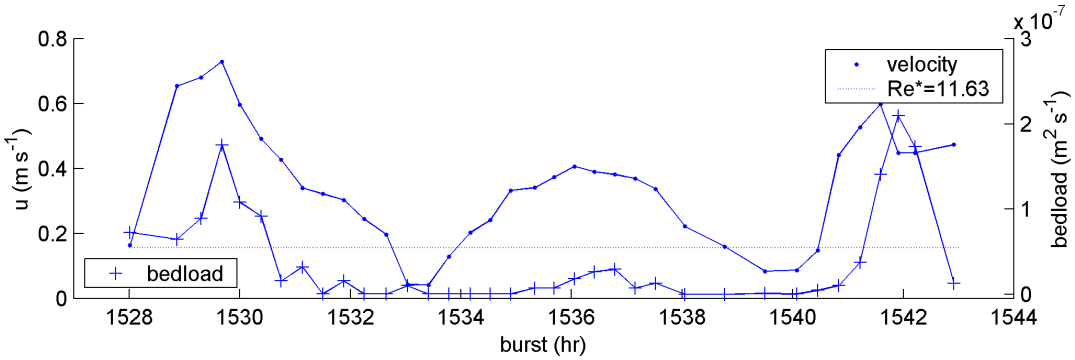

Figure 2 *First time series of bed load at N2, spring data, waves smaller than 0.5 m.Large velocity peaks are flood currents, smaller (middle) is ebb current.*

A typical time series of tidal current velocity and bed load transport (Figure 2) shows that significant sediment transport mostly occurs in the largest flood velocities. The bed load transport rates as a function of shear stress, both in dimensionless form, show a trend with a factor of 5 scatter (Figure 3). Below a dimensionless transport rate of 5 10^{-4} the scatter strongly increases, because this is a sampled bed load volume of about 1 ml in 20 minutes which is equal to the zero sampling volume. Dimensionless transports

below 5 10^{-4} are therefore not considered. Despite this scatter, the trend below and above the threshold is the same, as indicated by the moving average (computed in log space). The shear stress of the cloud just above the limit of measurable transport is about the critical Shields parameter for incipient motion (θ_{cr}=0.03).

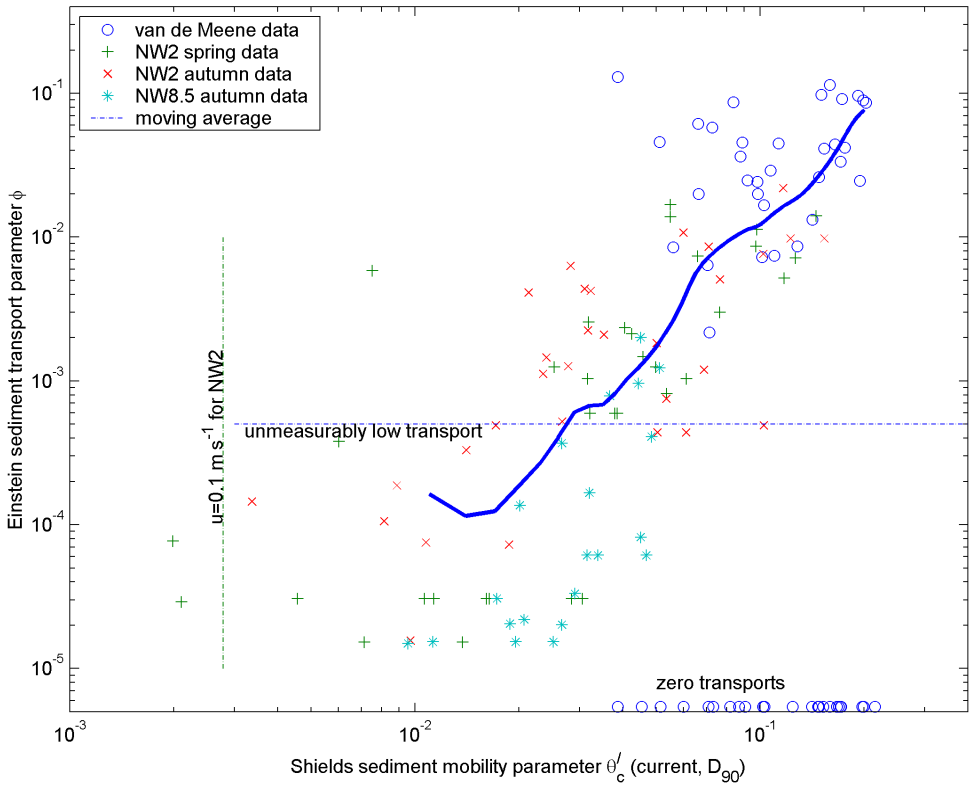

Figure 3 *Dimensionless bed load versus shear stress of the data and moving average. Limits of observability are given.*

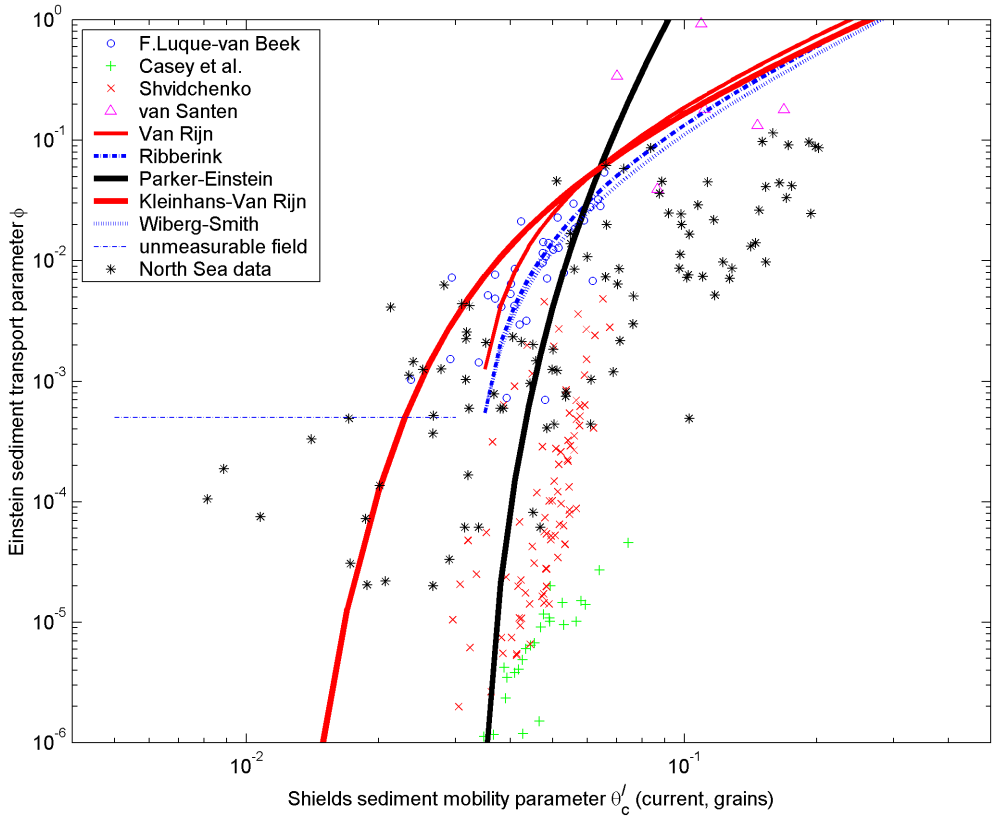

Figure 4 *Comparison of dimensionless transport data to other data and transport predictors (see Tables 2 and 3).*

4. REFERENCE SHEAR STRESS

It is useful to compare the present data to other datasets of bed load transport near incipient motion conditions (see Table 3 and Figure 4), even if these differ much in other respects such as grain size. The bed was nearly plane in all experimental conditions and the grain roughness is (assumed to be) D_{90}. The similarity collapse is done on the combined Noordwijk 8.5 and Zandvoort data because conditions are comparable, on the Noordwijk 2.2 datasets, and on the three datasets from literature separately. In addition, the critical Shields parameter for the D_{50} of each sediment is computed from the analytical Shields curve of Zanke (2003) for comparison (Table 4). The Zanke model accounts for the water depth effect that the Shields parameter significantly increases with $h/D_{50}<10$, which accounts for the rather large predicted critical Shields parameters of some laboratory data.
The well known scatter of empirical data on the Shields curve is caused by measurement errors, differences in criterion, etc. The empirical reference Shields values for the data from literature are both larger and smaller than predicted by the Shields curve (Table 4). The empirical reference Shields parameters of the North Sea data, on the other hand, are a factor of 2 smaller than the predicted values for the offshore data, and about a factor of 4 smaller for the shoreface data.

Table 3 *Experimental datasets of bed load near incipient motion of uniform sediment.*

Reference	D_{50} (µm)	remarks
Casey (1935, in Shvidchenko et al., 2001)	2460	35 experiments, only $h/D_{50}>10$
Shvidchenko et al. (2001)	1500–9000	86 experiments, only $h/D_{50}>10$
Fernandez-Luque and Van Beek (1976)	900, 1800, 3300	35 experiments, natural sediments

Table 4 *Reference shear stresses derived from the data.*

Dataset	empirical reference Shields	analytical critical Shields
Noordwijk 8.5, Zandvoort	0.039 ± 0.01	0.057
Noordwijk 2.2	0.017 ± 0.01	0.066
all North Sea data	0.027 ± 0.01	0.060
Casey et al.	0.083	0.073
Shvidchenko	0.060	0.056–0.08
Fernandez-Luque and Van Beek	0.019	0.035–0.055

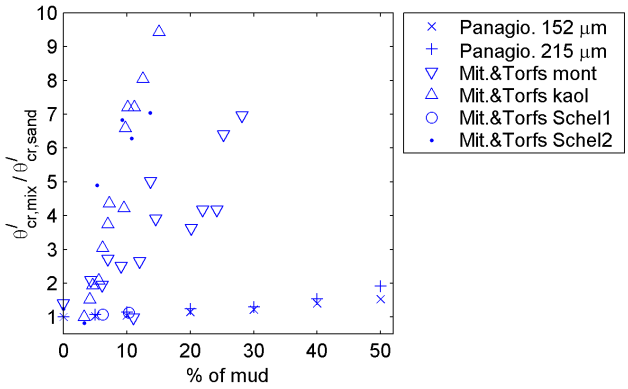

Figure 5 *Critical Shields parameter for varying % mud relative to the critical Shields parameter of clean sand. Data from Panagiopoulos et al. 1997 for given D_{50}, Mitchener and Torfs (1996) for artificial mixtures of sand plus kaolinite or montmorillinite and of mud from the Scheldt estuary at 1: the intertidal zone and 2: the subtidal zone. The compaction and lithology of the mixtures have not been taken into account which probably explains the lack of collapse.*

The reference (or critical) shear stress of sediment may be affected by various factors, for example the effect of the chosen grain roughness length, the calibration of the bed load sampler or the effect of cohesion due to mud in the sediment, cementation or compaction by benthic animals. The effect of chosen roughness length on empirical reference Shields values is limited to 20%, with $3D_{90}$ giving the largest dimensionless shear stress, $1D_{90}$ the smallest and $2.5D_{50}$ in between. (All data points shift along the x-axis with the same factor in Figure 3.) The reason is that the sediment has a narrow grain size distribution.

The effect of mud on incipient motion depends on the amount of clay in the sediment (mud to clay ratios are commonly 4:1), on the type of clay, on the compaction of the sediment and floc size of the clay and on the sand grain size (Mitchener and Torfs, 1996, Panagiotopoulos et al., 1997). The effect of the amount of clay is most easy to measure. For a mud fraction of 10% the increase in critical shear stress is between a factor of 1 and 8 (Figure 5). However, the Noordwijk sites have at most 5% mud in the bed. In addition, there is no difference between the bed load samplings done in spring and in autumn even though benthic fauna is absent in spring and abundant in autumn. Mud and biotic effects are therefore unlikely.

5. TEST OF BED LOAD PREDICTORS

The North Sea data are generally overpredicted with a factor of 5 by most predictors (Figure 4). Considering the scatter it is not useful to discuss the intricacies of these bed load predictors. The Parker predictor was found to predict well for gravel-bed rivers near incipient motion, but misrepresents the trend of the North Sea measurements. The empirical fit to the North Sea data is reported in Table 2. The comparison between the present data, the data from literature and the predictors demonstrates firstly that a universally valid predictor based on dimensionless shear stress only is not feasible, secondly that much of the data are on average below values of most predictors, and, thirdly that the present dataset is not exceptional compared to other datasets.

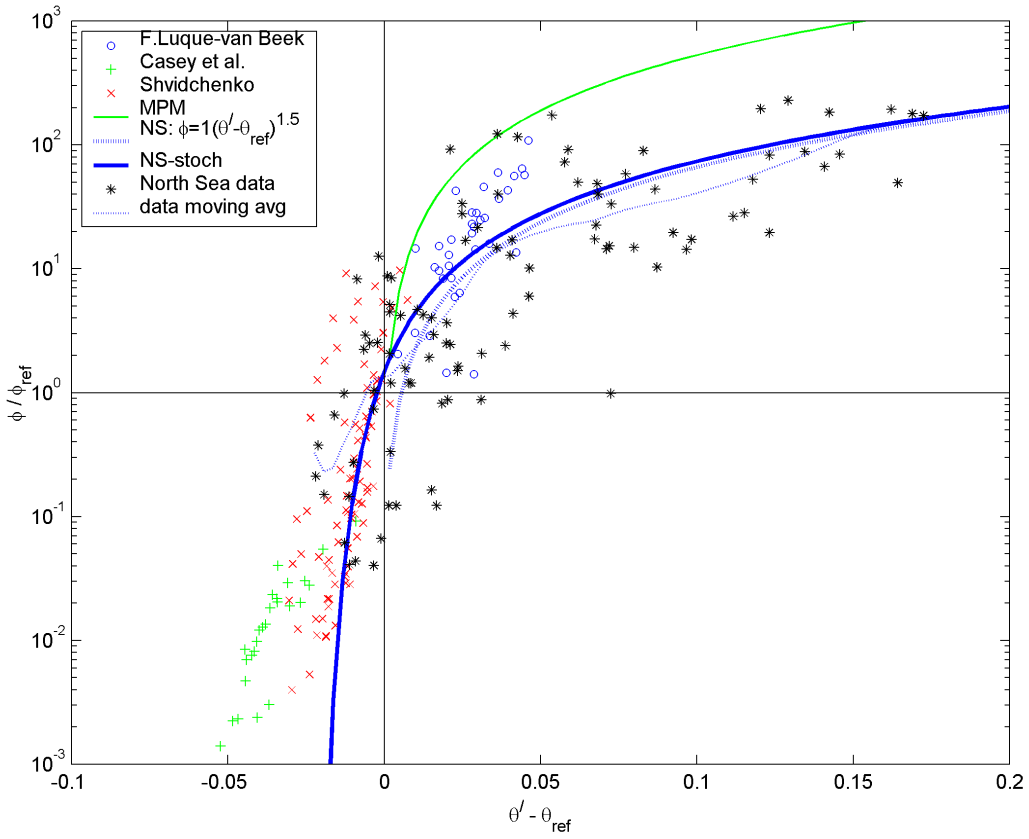

Figure 6 *Similarity collapse of the data. Dimensionless transport and Shields parameter are plotted relative to the critical/lowest measurable values. The stochastic version (method of Kleinhans and Van Rijn (2002) of the North Sea predictor predicts sediment transport below the critical Shields parameter. Note the difference between the Fernandez-Luque data and predictor, which is due to the different method and criterion for the computation of the critical Shields parameter.*

Moreover, all models except the stochastic predict zero transport below the chosen critical Shields parameter (Figure 4). However, the continuation of the trend of transport below threshold θ_{cr} shows that there is no real threshold but a gradual incipience region. This is due to the presence of near-bed turbulent τ fluctuations which exceed the 'threshold' even if the average near-bed shear stress is below the critical. Another factor is irregularities on the bed which cause protruding grains to be transported at a lower shear stress. For the Noordwijk site the time-averaged tidal τ is below critical for two-thirds of the time. However, the Kleinhans and Van Rijn (2002) predictor gives transports below the threshold for motion by virtue of turbulent fluctuations exceeding the threshold while the time-average shear stress is below the threshold (Figure 6). The effect of the stochastic module is that a significant transport rate is predicted below θ_{cr} in better

agreement with the measurements. The stochastical module is applied to the North Sea fitted predictor. Above θ_{cr} the stochastical predictor assymptotically approaches the non-stochastical predictor to which the stochastic module was applied. If a shear stress standard deviation of 0.28 rather than 0.4 were used then the transport predictor would be somewhat steeper below the critical Shields value. The new model fits reasonably well on the datasets for transport near incipient motion. This means that after accounting for differences in the critical Shields parameter, the North Sea stochastic predictor describes the data well.
It is not clear why the constant a=1 differs so much from existing predictors. The Wiberg-Smith correction clearly is not enough and mostly corrects at small Shields numbers whereas the deviation of the present data from the predictors is equally large for a range of Shields numbers. The error in the calibration of the Nile sampler is also not enough to account for the difference. Suppose the calibration factor is underestimated by a factor of 2, which is in conflict with the much better results in Gaweesh and Van Rijn (1994), then this still does not explain the factor of 5 deviation of sediment transport.

6. ANNUAL BED LOAD SEDIMENT TRANSPORT

To compute the alongshore annual bed load sediment transport, a probability distribution of depth-averaged current velocity is applied to the North Sea predictor. The correlation between velocities at a single height and the depth-averaged velocity derived from sensors between 0.05 and 1.1 m was used to compute an empirical probability distribution of depth-averaged current velocity from the year of data at the Noordwijk site. It is assumed that this probability distribution is representative for the shoreface and upper shelf. The probabilities for ebb currents (southward) are larger than for flood currents, but this is balanced by the larger peak velocities of flood currents.

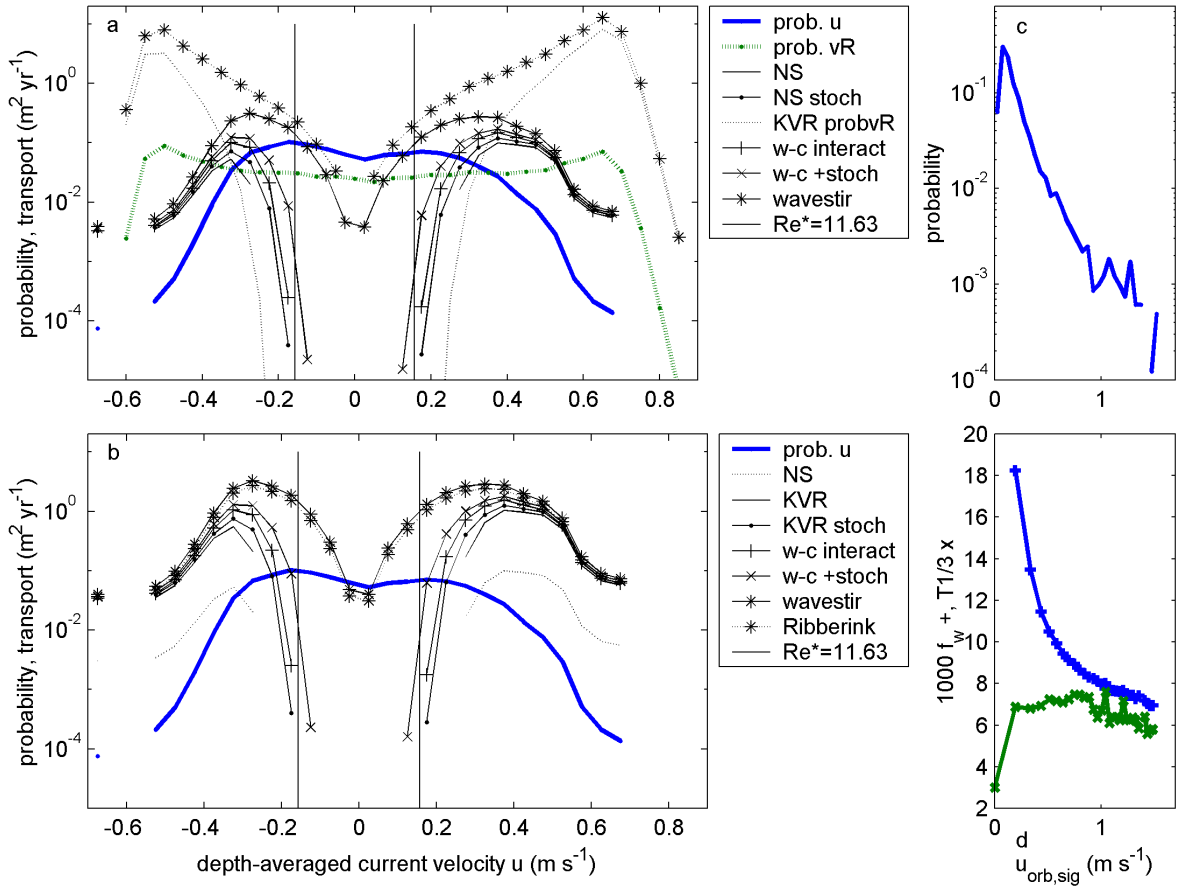

Figure 7 *a. Current climate at Noordwijk 2.2 and sediment transport predictions with the North Sea bedload predictor and with Kleinhans-Van Rijn (KVR) with the probability distribution of Van Rijn (transport in m^2 yr^{-1} per velocity bin). Positive current and transport are in the flood direction. b. Same, predictions with KVR and Ribberink (1998) for the measured climate. The (KVR) generally overpredicts a factor of 10 compared to the North Sea (NS) predictor. c. Orbital flow climate at Noordwijk 2.2. d. Average friction factor (multiplied with 1000) and T1/3 period of the orbital velocity classes in c.*

The sediment transport associated with each class of velocity, multiplied with the probability of that class, is the largest for the flood currents (Figure 7, Table 5). The computations are given for the North Sea predictor

and the Kleinhans and Van Rijn (2002) predictor, both with and without the stochastical module. Intra-tidal water level variations are ignored which can safely be done as the variations are at most 10% while water depth only affects the results through the roughness predictor. The transport by flood currents is 4-5 times larger than by ebb currents. The Van Rijn predictor yields about 10 times larger transports than the North Sea predictor in all cases as can be expected from the difference between the predictors. The stochastical predictors yield 25% more transport than the deterministical in the flood direction, and 40% in the ebb direction. The effect on the net transport is only a 14% increase due to the opposing effect of the strongly increased ebb transport in the stochastic mode.
The computations are also given including the effect of wave-current interaction (Figure 7, Table 5), assuming the wave direction to be perpendicular to the currents. This is reasonable because the tidal currents are parallel to the shoreline whereas the significant waves come from directions between north-west and south-west. The effect of wave-current interaction is a 55% increase of transport in the flood direction, 110% in the ebb direction and 25% in the net transport. Surprisingly, the combined effect of wave-current interaction and stochastic flow variations is much larger than that of wave-current interaction only: for flood, ebb and net transport respectively, a 90%, 190% or 40% increase of transport on the basic prediction, and a 22%, 40% or 10% increase relative on the prediction with wave-current interaction.
The effect of wave stirring on the flood and ebb transports is 2-3 times as large as wave interaction and turbulence combined, which is important for infilling of sand extraction pits. However, the net transport is about equal.
Summarising, the effect of wave-current interaction on flood or ebb transports is a factor of 2 larger than the effect of stochastic flow variations, and the effect of wave stirring again is a factor of 2-3 larger. The latter is not surprising, because the transport is very near or below incipient motion for most of the time in the ebb current, so enhanced mobility will have a large effect. However, the net transport is not affected much by any model extension.

Table 5 *Comparison of computed annual bed load transports at Noordwijk 2.2 km offshore for the Van Rijn and North Sea predictors with all combinations of stochastic and wave-current interaction modules (integration of Figure 7). The computation for the pdf of depth-averaged velocities in Van Rijn et al. (this volume) is given in the last three columns.*

	m^2 yr^{-1}	w-c Soulsby (1997) stirring Ribberink (1998)			Van Rijn current velocity pfd		
Predictor	module	Flood	Ebb	Net	Flood	Ebb	Net
Van Rijn (1984)	basic	4.43	-1.37	3.06			
	stochastic	5.49	-2.04	3.45	23.61	-8.40	15.21
	w-c interaction	6.81	-2.97	3.84			
	w-c + stochastic	8.32	-4.09	4.23			
	wave stirring Rib98	17.09	-12.82	4.27	44.88	-25.32	19.56
Ribberink (1998)	wave stirring Rib98	14.20	-10.49	3.71	37.98	-21.04	16.94
North Sea	basic	0.42	-0.13	0.29			
	stochastic	0.52	-0.19	0.33	2.27	-0.81	1.46
	w-c interaction	0.65	-0.29	0.36			
	w-c + stochastic	0.80	-0.39	0.41			
	wave stirring Rib98	1.64	-1.23	0.41	4.31	-2.43	1.88

Van Rijn et al. (this volume) estimated the annual net sediment transport rate at a water depth of 20 m at 10 m^2 yr^{-1}. This value is three times larger than the net transport estimated here with the predictor of Van Rijn (1984). The cause is that Van Rijn used a different probability density function for depth-averaged tidal currents, in which the flood duration is equal to the ebb duration and the velocity magnitudes are larger. This contradicts the measurements presented here. Using the present predictors and the pdf of van Rijn, indeed 3-5 times larger flood and ebb transports and five times larger net transport are found (table 5). This is a much larger effect than of any model extension.

7. CONCLUSIONS

Bed load transport rates in field conditions near incipient motion are notoriously difficult to measure and predict. Despite the large scatter a trend was observed of measured transports of a factor of 5 smaller than common models predict. This is consistent with datasets from literature of bed load transport very near

incipient motion. The factor 5 cannot be explained with effects of cohesion due to mud or errors in instrument calibration.
An empirical North Sea predictor was derived from the data after removing effects of different critical Shields parameters for the beginning of measurable bed load transport: $\phi=1(\theta-\theta_{cr})^{1.5}$. Predictions improved when the variations of shear stress due to turbulence are included in this model stochastically. Predicted annual current-related bed load transport increases with about 20% due to the stochastic module. The effect of wave-current interaction on this annual transport rate is about twice as much as the stochastic flow variations. The combined effects have the largest effect on the ebb current. Since the flood velocities are larger than the ebb velocities, the net transport also increases with the addition of both effects. The effect of wave stirring on flood or ebb transports is again twice as much although the net transport is not affected. Choosing a different bed load predictor or a less accurate representation of the tidal current climate will, however, lead to much larger bias than ignoring the turbulence, wave-current interaction and wave stirring effects.

8. REFERENCES

Fernandez-Luque, R. and Van Beek, R. 1976. Erosion and transport of bed-load sediment, J. Hydraulic Research 14(2), pp. 127-144.
Gaweesh, M.T.K. and Van Rijn, L.C. 1994. Bed-Load Sampling in Sand-Bed Rivers, J. of Hydraulic Engineering 120, 1364-1384.
Kleinhans, M.G. and Van Rijn, L.C. 2002. Stochastic prediction of sediment transport in sand-gravel bed rivers, J. of Hydraulic Engineering 128, 412-425.
Madsen, O.S. and Grant, W.D. 1976. Sediment transport in the coastal environment. MIT Ralph M. Parsons Lab., Report 209, Cambridge, USA.
Meyer-Peter, E. and Mueller, R. 1948. Formulas for bed-load transport, 3rd Conf. Int. Assoc. of Hydraul. Res. Stockholm, Sweden, 39-64.
Mitchener, H. and Torfs, H. 1996. Erosion of mud/sand mixtures. Coastal Engineering 29, 1-25.
Panagiotopoulos, I., Voulgaris, G. and Collins, M.B. 1997. The influence of clay on the threshold of movement of fine sandy beds. Coastal Engineering 32, 19-43
Parker, G., Klingeman P.C. and McLean D.G. 1982. Bedload and size distribution in paved gravel-bed streams. J. of the Hydr. Div., ASCE, 108(HY4) , 544-571.
Ribberink, J.S. 1998. Bed-load transport for steady flows and unsteady oscillatory flows, Coastal Engineering 34, 59-82
Shvidchenko, A. B., Pender, G. and Hoey, T. B. 2001. Critical shear stress for incipient motion of sand/gravel streambeds. Water Resources Research, 37, 2273-2283
Soulsby, R. 1997. Dynamics of marine sands. Thomas Telford Publications, London, United Kingdom.
Van de Meene, J.W.H. 1994. The shoreface-connected ridges along the central Dutch coast, Royal Dutch Geographical Society, Netherlands Geographical Studies 174, Utrecht, The Netherlands
Van Rijn, L.C. 1984. Sediment transport, part I: bed load transport, J.of Hydraul. Eng. 110(10), 1431-1456.
Van Rijn, L.C. 1997. Sediment transport and budget of the central coastal zone of Holland. Coastal Engineering 32, 61-90.
Wiberg, P. L. and Smith, J. D., 1989. Model for calculating bed load transport of sediment. J. of Hydraulic Engineering 115, 101-123.
Zanke, U.C.E. 2003. On the influence of turbulence on the initiation of sediment motion, International J. of Sediment Research 18(1), 1-15.

9. ACKNOWLEDGEMENTS

Rijkswaterstaat Directorate North Sea, the Vliestroom and Zirfaea crews are thanked for their efforts to make the Nile sampler measurements possible. Leo van Rijn, Richard Soulsby, Jan Ribberink and Piet Hoekstra are thanked for discussion. Jan van de Meene is thanked for providing his data. Lobke Haaring is acknowledged for her BSc work on incipient motion of sand-mud mixtures. Funded by EC MAST, MAS3-CT97-0086.